

# EARTHQUAKE STRONG MOTION DURATION: UNIFYING CRITERIA FOR DEFINITION AND A NEW METHOD TO CALCULATE IT

Heriberto Echezuría  
[hechezuria51@gmail.com](mailto:hechezuria51@gmail.com)

Centro de Investigación y Desarrollo de Ingeniería (CIDI). Universidad Católica Andrés Bello. Caracas, Venezuela.

Historia del Artículo  
Recibido 15 de Septiembre de 2017  
Aceptado 15 de Septiembre de 2017  
Disponible online: 20 de Septiembre de 2017

**Abstract:** Values of strong motion duration  $T_{sm}$  and intensity  $I_{sm}$  show a significant variation depending on the definition used to estimate them. In this article comparisons are made of definitions given by Vanmarcke-Lai; Bolt, Trifunac-Brady and McCaan-Shah using 83 accelerograms of 18 earthquakes with magnitudes ranging from 5 to 7.7. Strong motion intensities, i.e. the energy yielded by the strong section of the records, were estimated taking the square of the root mean square of ground acceleration ( $a_{rms}^2$ ), denominated the “power” of the record, times the duration of the strong section of the record in seconds,  $T_{sm}$ , i.e.  $I_{sm} = a_{rms}^2 T_{sm}$ . It had been reported that even though durations in seconds and root mean square of ground acceleration values resulted quite different among those four definitions, strong motion intensities resulted relatively close to each other. This unexpected result for real accelerograms was studied in detail for simple and complex time histories obtained with Fourier concepts for which strong motion intensities were estimated. Analyses indicated that all definitions involved the same sectors of the accelerograms but differ in defining the beginning and ending point. In this article, new criteria to unify the definition of strong motion duration and a new method to calculate it are proposed. The new method is based on variation of both, the strong motion intensity and the power of the acceleration record with duration and it yields a unique duration for the record. It will also allow treating the motion intensity as a real demand variable and calculating its hazard which improves the way to assess liquefaction potential.

**Keywords:** Strong ground motion intensity, Arias intensity, attenuation of seismic parameters, earthquake energy, earthquake duration, root mean square of acceleration, cyclic stress ratio, cyclic resistance ratio, liquefaction.

## Duración del Sector Fuerte del Terremoto: Unificación de Criterios para Definirla y Nuevo método para Calcularla

**Resumen:** Los valores de la duración,  $T_{sm}$  y la intensidad  $I_{sm}$  del sector fuerte del acelerograma muestran variaciones significativas dependiendo de la definición de duración empleada. En este artículo se comparan esas dos variables utilizando las definiciones de Vanmarcke-Lai; Bolt, Trifunac-Brady and McCaan-Shah aplicadas a 83 acelerogramas de 18 terremotos con magnitudes de momento entre 5 y 7.7. La intensidad del sector fuerte, es decir, la energía, fue estimada a partir del producto del cuadrado del error medio cuadrado de la aceleración, ( $a_{rms}^2$ ), denominada la “potencia”, por la duración en segundos;  $T_{sm}$ , o sea,  $I_{sm} = a_{rms}^2 T_{sm}$ . Se ha comprobado que, a pesar de que la duración y el error medio cuadrático resulten muy distintos entre si con las cuatro definiciones, las intensidades del sector fuerte resultan bastante similares entre si para esas definiciones. Este resultado inesperado par acelerogramas reales fue estudiado en detalle utilizando funciones periódicas simples y otras complejas obtenidas aplicándoles criterios de Fourier y escalamiento. Los resultados indican que todas las definiciones de duración envuelven el mismo sector del acelerograma pero difieren en la forma de seleccionar su inicio y su final. In este artículo, se presentan nuevos criterios y un nuevo método para unificar la definición del sector fuerte del sismo. El nuevo método se basa en la variación de ambas, la intensidad del sector fuerte del acelerograma y la potencia del mismo con la duración y el mismo provee una definición única de la duración. Ese nuevo método también permite el tratamiento de la intensidad del sector fuerte como una demanda real a la cual puede calcularse la amenaza y permite mejorar la forma de evaluar el potencial de licuación.

**Palabras Clave:** Fuerte intensidad de movimiento en el suelo, intensidad de Arias, atenuación de parámetros sísmicos, energía sísmica, duración de terremoto, cuadrado medio de aceleración, relación de tensiones cíclicas, relación de resistencia cíclica, licuefacción.

I. INTRODUCCIÓN

It is well known that peak ground acceleration (PGA) is not a reliable variable to indicate the amount of damage an earthquake can induce to a structure or to a soil mass because it does not take into consideration strong motion duration. It is illustrated in the upper part of Fig. 1, where both acceleration records included have about the same PGA but exhibit quite different durations. It is evident that the record on the right will cause a larger damage than the one on the left.

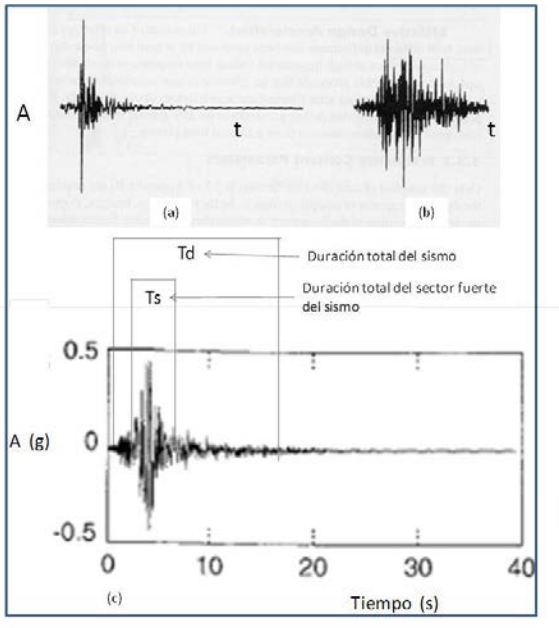


Figure 1. Above, two ground motion records with about the same PGA but different duration. Below, indication of the strong section of the record.

Thus, when one needs to consider the energy of the quake it has been customary to refer to the magnitude because it allows assigning a number of cycles of equivalent amplitude. The problem with this approach is that the characteristics of the ground motion for a given magnitude vary with distance. Thus one should also have to indicate the distance as well as the magnitude to properly establish the number of equivalent cycles of a given earthquake. An alternative way to solve this problem is by defining the duration of the strong section of the acceleration record, as indicated in the lower part of Fig. 1. In this way, the intensity

or energy of the strong part of the acceleration record is completely defined.

In order to define the strong part of the acceleration record, the root mean square of the acceleration record,  $a_{rms}$ , can be used. In Fig.2 it is shown a digitized acceleration record which becomes a sequence of individual or discrete values of acceleration with time and the process to define its root mean square.

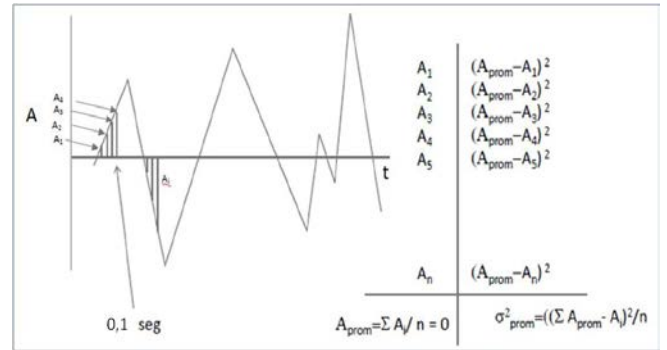
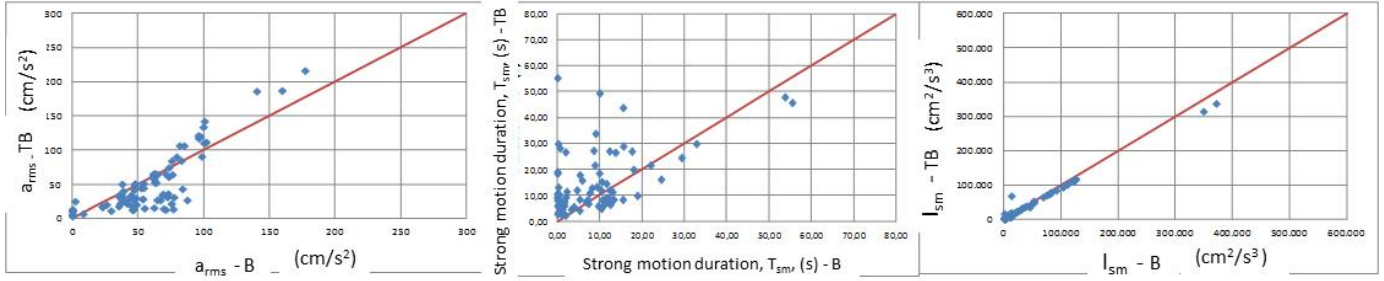


Figure 2. Digitized acceleration record showing the sequence of individual or discrete values of acceleration from which the root mean square of such values can be obtained.

As will be presented in the next section,  $a_{rms}$  values have been used, either directly or indirectly, by several authors to try to define the strong section of an acceleration record. Other authors have attempted to define the strong section of the accelerogram based on other criteria. The point is that, as will be discussed later in this article, each available definition of strong motion yields different duration in seconds as well as different  $a_{rms}$  values, as reported by Echezuría [1] for four definitions of strong motion i.e. Vanmarcke-Lai (VL) [2]; Bolt (B) [3], Trifunac-Brady (TB) [4] and McCaan-Shah (McS) [5].

Despite such situation, Echezuría [1] also found that even though the values of  $a_{rms}$  and duration,  $T_{sm}$ , obtained for strong part of the accelerograms with the four definitions mentioned above were very different between each other, the values of the strong motion intensity or energy were very similar. This can be seen in Fig. 3 where  $a_{rms}$ ,  $T_{sm}$  and  $I_{sm}$  from TB y B definitions are compared for the data used in this article. The

way how the strong motion intensity was calculated will be indicated later in this article.



**Figure 3. Comparison of  $a_{rms}$ ,  $T_{sm}$  and  $I_{sm}$  obtained from the TB and B definitions applied to the earthquake included in the data base of this article. Echezuría [1].**

Notice the dispersion in the values of  $a_{rms}$  and  $T_{sm}$  but how well the values on intensity  $I_{sm}$  correlate between each other for these two definitions. Nevertheless, it is worth mentioning, that Bolt's definition of duration does not work well for moment Magnitudes lower than 6.5 for which no duration is obtained in some cases given the amplitudes selected for the definition. Other comparison among the rest of the definitions can be found in Echezuría [1].

The closeness among the different values of intensities was an unexpected finding considering the diversity of criteria used to define the duration of the strong part of an accelerogram. Further discussion on the criteria used for the different definitions as well as on the shape of the functions of the intensity or energy, the  $a_{rms}$  and  $a_{rms}^2$  will also be presented later on this article.

## II. BRIEF DESCRIPTIONS OF THE FOUR DEFINITIONS OF STRONG MOTION AND DATA BASE

Arias [6] proposed a method to evaluate the energy dissipated during strong ground motion given by:

$$I_a = \int_0^\infty E(\omega) d\omega \dots(1)$$

where,  $I_a$  is the Arias intensity, and,  $E\omega$  is the energy dissipated by an oscillator with natural frequency,  $\omega$ . Note that the Arias intensity uses

the total duration of the record. See Fig. 1. It can be shown that, when applied to an acceleration time history along with the power spectral concept the expression above can become:

$$I_a = a_{rms}^2 T_d \dots(2)$$

where,  $a_{rms}$  is the root mean square of the acceleration time record, and  $T_d$  is the total duration of the record in seconds. The expression above indicates that the mean square of the ground acceleration can be taken as an average constant intensity acting during the total duration  $T_d$  of the motion.

Vanmarcke and Lai (VL) as well as Trifunac and Brady (TB) used Arias intensity ( $I_a$ ) in their definitions of duration. Trifunac and Brady defined the beginning of the strong motion section of the accelerogram as the time at which 5% of the  $I_a$  is reached and the end as the time which yields 95% of the  $I_a$ . Justification for this is that most earthquakes have low amplitude intervals early and late in the record.

Vanmarcke and Lai defined the duration based on the assumption that the  $I_a$  is uniformly distributed at a constant average power given by  $a_{rms}^2$  over the strong ground motion interval,  $T_d$ . Further, those investigators assumed that the time history of acceleration is a Gaussian process and defined the relationship between peak ground acceleration PGA and  $a_{rms}$ , as  $Q=PGA/a_{rms}$ . In addition, VL took arbitrarily the probability of exceeding at least once the ratio, Q, during the time interval,  $T_{sm}$ , as  $1-e^{-1}$ . Under these conditions the solution for  $T_{sm}$  can be obtained in terms of  $I_a$ ,  $T_{sm}$ , PGA and  $T_0$ , as follows:

$$T_{sm} = Q^2(I_a/PGA^2) = [2\ln(2T_{sm}/T_o)][I_a/PGA^2]$$

For  $T_{sm} \geq 1.36 T_o \dots(3)$

And

$$T_{sm} = Q^2(I_a/PGA^2) = 2I_a/PGA^2$$

For  $T_{sm} < 1.36 T_o \dots(4)$

where,  $T_{sm}$  is the duration of the strong motion and  $T_o$ , is the average period of the record. However, considering the arbitrariness of the selection of the probability of exceeding the, Q-ratio, during the time,  $T_{sm}$ , as well as the fact that they have found the ratio of  $I_a/PGA^2$  to be close to linear, VL proposed a simplified version of the solution using a constant value for the ratio, Q-ratio = 2.74. This simplified version was used in this study. The center of the duration corresponds to the location of the PGA and half of it is then taken towards the upper portion and the other half towards the lower portion.

McCaan and Shah defined the strong section of the accelerogram as the interval which exhibits a constant  $a_{rms}$  level. The beginning of the strong motion is obtained by forming the cumulative root mean square of the ground acceleration function of the reversed accelerogram and selecting the time at which the root mean square of the ground acceleration begins a steady decline. This time defines the beginning of the strong section and is denoted as,  $T_1$ . The end of the strong section is obtained by applying the same method to the original accelerogram starting at,  $T_1$ .

Bolt used a threshold value concept in order to define the strong part of the accelerogram. Once a threshold value of the acceleration is defined according to the phenomenon under study, the strong part is the enclosed portion between the first and last time the threshold is exceeded along the acceleration record. In this study a value of the acceleration of 0.05 g was used. Note that, g, is the acceleration of gravity in centimeters per squared seconds. There are some other definitions of duration, such as: Boore (1983), Perez (1974) and Trifunac and Westermo (1977), fide Kramer [7]. Nevertheless, the four definitions previously described are the most widely used. In particular the one by Bolt given its simplicity.

Echezuría [8] studied in detail the shape of the of  $a_{rms}$ ,  $a_{rms}^2$  and intensity,  $I_{sm}$  functions with duration from simple harmonic functions as well as from complex ones resulting from applying Fourier concepts to the harmonic ones, to understand the factors that influence them. Later, the criteria resulting from such analysis were compared with those used in the four definitions of duration under study to come up with unifying criteria regarding the definition of the strong part of an accelerogram.

The strong section of the accelerogram was defined by Echezuría [1, 8] with the following equation:

$$I_{sm} = a_{rms}^2 T_{sm} \dots(5)$$

According to eq. 5, Echezuría uses a definition of the strong motion very similar to that given by eq. 2. It implies that the energy released by the quake represents an intensity that can be obtained from an average power given by  $a_{rms}^2$  acting over the strong motion duration,  $T_{sm}$ . There is another definition of quake intensity given by Ang (1990), fide Kramer [7] which is linearly related to an index of accumulated structural damage due to maximum deformations and absorbed hysteretic energy. It is the Characteristic Intensity which has the following expression:

$$I_c = a_{rms}^{1.5} T_d^{0.5} \dots(6)$$

Notice that this definition of intensity uses the total duration of the quake. This definition will be explored in future work. This article uses only the definition of intensity given by eq. 5.

## 2.1 Composition of the data base used in the study

The data base used in this study includes a total of 83 accelerograms from 18 earthquakes with moment magnitudes between 5 and 7.7, as depicted in Table A-1 of Appendix 1. This data base includes records obtained in the near field, that is, less than 10 km of the fault. The distance definition, R, used in the study corresponds to the closest distance to the surface projection of fault rupture area. The  $a_{rms}$  values were calculated using the four definitions of duration mentioned above, i.e. V-L; B, TB and McS.

In the meantime, the author prepared a series of artificial functions of acceleration with time. Some were based on simple harmonic functions and others were obtained as the summation and escalation of several of the simple function, as indicated by Poisson criteria. These functions are not explicitly included in the article, but the result for some of them indicating the point expressed in the text.

III. SHAPES OF  $a_{rms}$ ,  $a_{rms}^2$  AND  $I_{sm}$ , FUNCTIONS AND UNIFICATION OF CRITERIA TO DEFINE DURATION OF STRONG MOTION

As mentioned above, Echezuría [8] studied in detail the shape of the of  $a_{rms}$ ,  $a_{rms}^2$  and intensity,  $I_{sm}$  functions with duration to understand the factors that influence them. The intention was to come up with unifying criteria regarding the definition of the strong part of an accelerogram.

Typical complex functions used in this analysis are shown in Fig. 4. These are found similar to real earthquakes. Simple periodical functions used are of the form  $A \cos(\omega t)$  y  $A \sin(\omega t)$ , where, the frequency and, t, the time, as depicted in Fig. 5.

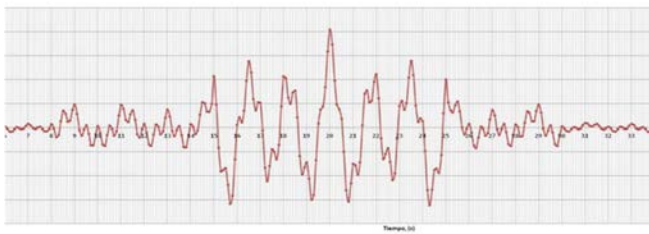


Figure. 4 Complex function obtained by adding and scaling periodical simple functions using Fourier concepts.

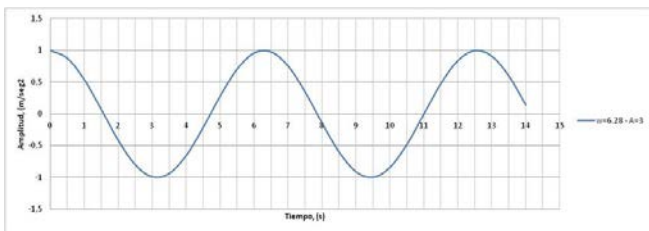


Figure. 5 Typical harmonic function of acceleration with time.

The calculation of  $a_{rms}$ ,  $a_{rms}^2$  and  $I_{sm}$  functions were conducted; first, starting from the PGA. In this way the duration was equally distributed at both sides of it. The three functions to define the record intensity were calculated considering all the acceleration values contained within each duration evaluated. The process was as follows, first the PGA was located, then increasing values of the duration using the time interval applied to digitize the time records was,  $\Delta t=0.1s$ , was used to calculate the  $a_{rms}$ ,  $a_{rms}^2$  and  $I_{sm}$  values. A graph of those three variables was prepared with increasing duration and their shapes were analyzed. Note that  $\Delta t=0.1s$  is the same time interval utilized to digitize real earthquakes.

The other way of calculating the three functions indicated above, was conducted starting from the beginning of the records and function shapes were compared with the ones starting from PGA. It turned out that variable functions had similar shapes for both methods.

Echezuria [8] found that for any given acceleration time record, either harmonic or complex or real, the  $a_{rms}$  and the  $a_{rms}^2$  functions reach a maximum and then start to decrease. Afterwards, a series of maximums and minimums occur depending on the amplitude of the accelerations values included in any given time span. This implies that between two consecutive maximum and minimum there exists a slope. The shape of the  $a_{rms}^2$  function is identical to the shape of the  $a_{rms}$  function but the amplitudes of the function are much higher in the former. Similarly, the slope between two consecutive maximum and minimum are also higher in the  $a_{rms}^2$  function than in the  $a_{rms}$  function. This can be seen in Figure 6 for a harmonic function, left, and for a complex function of acceleration with time, right.

When the acceleration values are similar to each other the calculated  $a_{rms}$  values increase slowly as duration increases. This is due to the fact that the newly involved values of acceleration are no so different from the PGA and the  $a_{rms}$  grows

slowly. As time span increases the newly incorporated acceleration values start to differ more from the PGA and the  $a_{rms}$  becomes larger. This can be seen for the harmonic acceleration time record shown on the left of Figure 6.

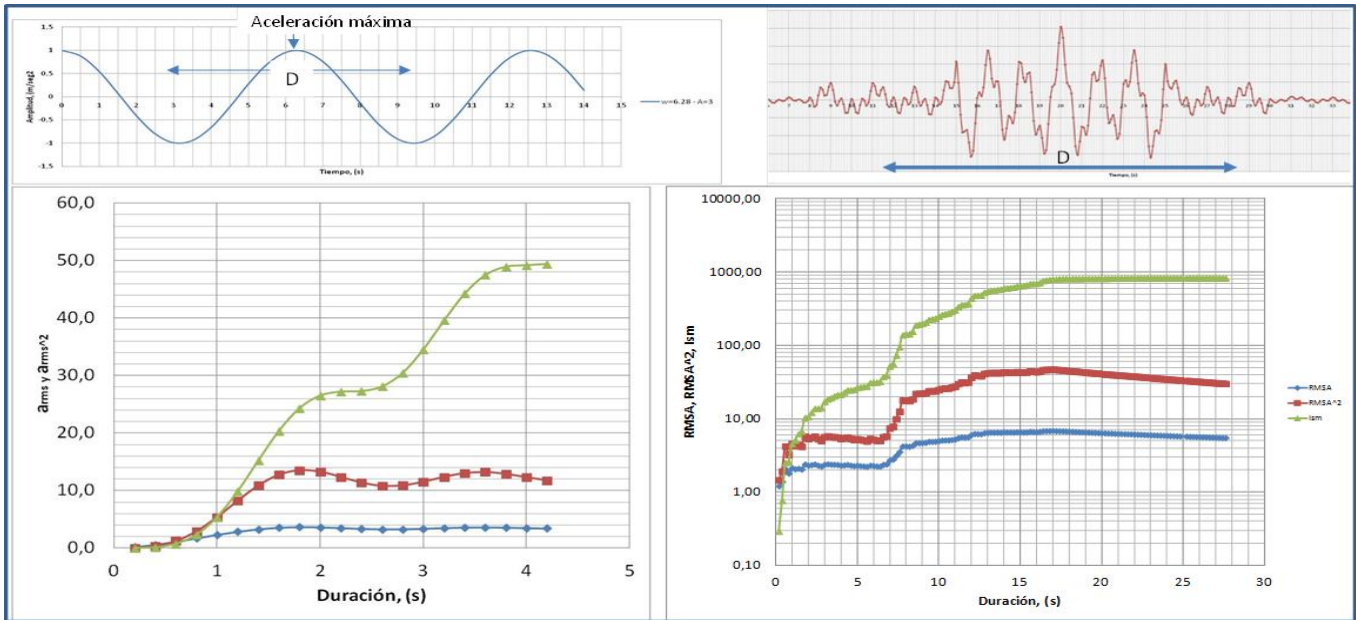


**Figure 6. Constant growing of the  $I_{sm}$  (energy) for a harmonic and complex acceleration functions indicating the duration of strong motion. Echezuría [8].**

However, if the acceleration values nearby the PGA differ significantly from each other and the PGA itself, as in the case of an irregular acceleration record or one from an earthquake, such as the one shown on the right of Figure 6, the calculated  $a_{rms}$  values increases rapidly, as duration increases. Later, as the acceleration values incorporate more peaks with values approaching the PGA, the calculated  $a_{rms}$  values start to reduce. This can be seen in Figure 6. Note; however, that in both cases, the intensity always increases even though both, calculated  $a_{rms}$  and  $a_{rms}^2$  values may decrease.

Notice that even though the intensity always increases, the rate at which it raises changes depending on the behavior of the  $a_{rms}^2$  function behavior. It can be seen that in both cases included in Figure 6, the slope of the intensity changes drastically from a fast increase to a slow one whenever the values of  $a_{rms}^2$  change its rate of growth or decrease after increasing. Thus, these changes in the slope of the intensity along with a

sustained decrease in the  $a_{rms}^2$  function define both the entrance and the exit to the strong part of the acceleration record.

For the harmonic function in the left of Figure 6 every quarter of a cycle a maximum is reached for the  $a_{rms}^2$  function followed by a drastic reduction. This process repeats itself which means that there will be two more maximums added to the two included in Figure 6 before the whole process repeats for the next cycle. Note that Figure 6 only depicts almost a half of a cycle.

For the irregular function on the right of Figure 6 the first change is seen at 1s as expected due to the rapid change in the acceleration values at both sides of the PGA. Then there occur several changes in the slope of the  $a_{rms}^2$  function up to 17 seconds. After that value, there is a sustained decrease of the  $a_{rms}^2$  function coinciding with the slower increase of the slope of the intensity function. It is this last change of both the  $a_{rms}^2$  and intensity functions which defines the duration of the strong section of the acceleration record. In other words, the strong motion duration is 17 seconds centered at the PGA, that is, 8.5s at each side of it.

It was also studied the influence of the amplitude of the accelerations in the vicinity of the strong section. This can be seen in Figure 7 where two records with different values at the entrance of the strong section are compared. In this case, the  $a_{rms}^2$  values were also calculated starting from the PGA. It can be seen that the larger the difference in amplitudes of the accelerations

outside but near the strong section with the amplitudes within the strong section the smaller the growing slope of the intensity. Notice that the difference between the two records included in Figure 7 is that the one on the left has transition or intermediate values at the entrance and at the end of the strong section whereas the one on the right has only at the end.

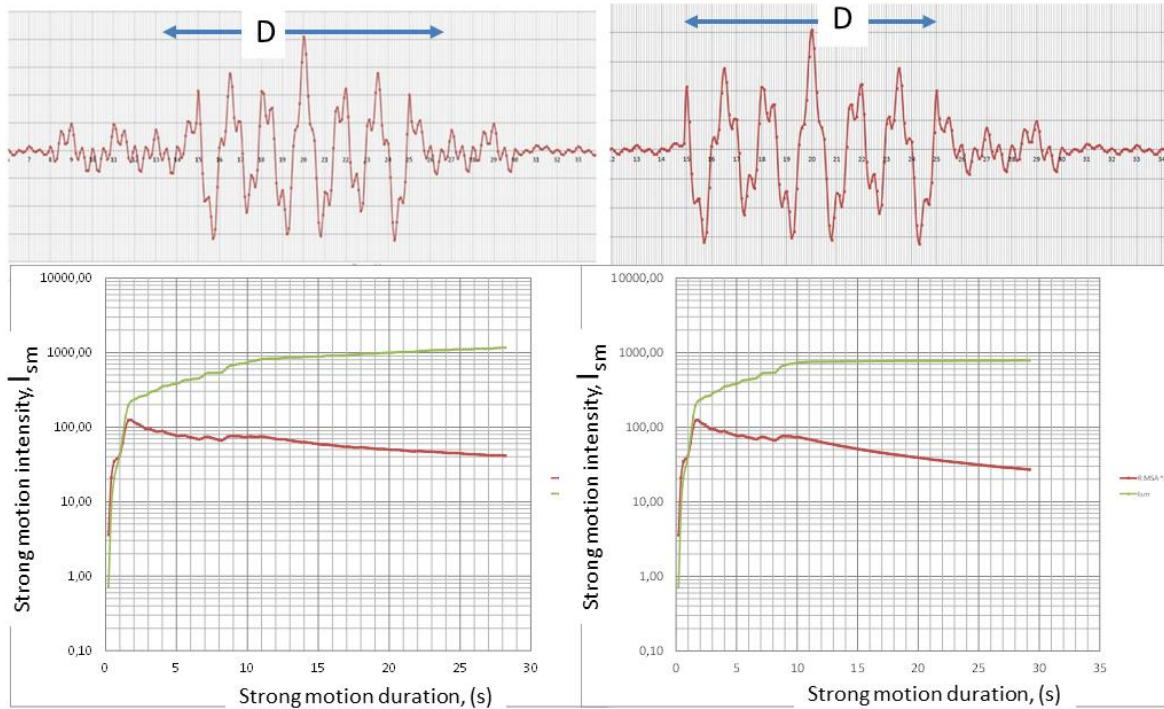


**Figure 7. Comparing the  $I_{sm}$  and  $a_{rms}^2$  of the strong sections of two different complex functions of acceleration with duration.**

For the case on the left of Figure 7, the last change of the intensity slope that coincides with a sustained reduction of the power function occurs at 13 seconds. Thus, the duration is 13s evenly distributed around the PGA which means that strong motion starts at 13,5s and ends at 26.5s. For the record on the right of Figure 7, the last change in the intensity slope coinciding with the steady decline of the power function occurs at about 10s. So, in this case the strong part starts at 15s and ends at 25s.

It is worth mentioning that if the calculation of the  $a_{rms}^2$  and intensity functions was started from the beginning of the record, the first and last changes in slope must be identified to define the span of the strong part of the record. It is simpler working

from the PGA as only the last change in slope has to be identified to define the strong section of the record.

#### IV. ASSESSING THE BEHAVIOR OF THE STRONG MOTION DURATION FOR THE FOUR DEFINITIONS USED IN THIS ARTICLE.

It can be seen in Figure 8 a typical curve of the Arias Intensity ( $I_a$ ) for a given earthquake. One shall remember that the expression of the Arias Intensity also uses the  $a_{rms}^2$  (see eq. 2) as the power, which implies that it must have a similar tendency as the red curve on the right of Figures 6 and 7. That is, it will amplify the variations of the  $a_{rms}$  function and show the minimal growing slope of the intensity function coinciding with a decrease of power.

Consequently, if one identifies the changes in slope of the  $I_a$  curve the changes in slope will indicate where the decrease of the power function occurs. The changes in slope of the  $I_a$  are depicted with straight lines in Fig. 8 for this particular case. In addition, two circles have been also included to identify the first and last slope change of the intensity.

Similarly, it is also shown in Figure 8 the definition of the TB strong motion duration. Thus, the location of 5% and 95% values of  $I_a$  are indicated with dashed lines. It is worth mentioning that those two values which define the TB duration are not necessarily related to the changes in the slope of the  $I_a$  function but they appear to be close to them.

On the other hand, it was previously mentioned in Section 2 of this article, the McS strong motion definition uses the first changes in the slope of the  $a_{rms}$  function that indicate a steady decline. As can be seen in Fig. 7, the first change implying a decline in the power or the  $a_{rms}$  function does not represent the maximum energy delivered by the acceleration record. In the case of the Arias Intensity function of Figure 8, the end of McS definition would probably be identified with the change of slope occurring at 75% of  $I_a$ . The beginning of the strong motion is identified starting the  $a_{rms}$  function from the previously identified end in reverse way. It would most probably coincide with the first slope change at about 10% of  $I_a$ .

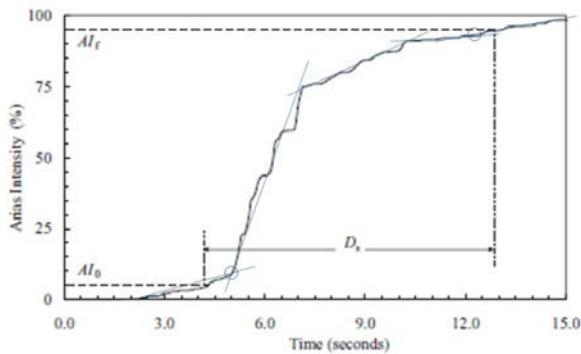


**Figure 8. Slope changes of the Arias Intensity ( $I_a$ ) for a typical earthquake and definition of the TB strong motion section.**

Consequently, the McS definition would underestimate the strong motion section of the accelerogram. This is confirmed in Figure 9 (Echezuría [1]) where  $I_{sm}$  values from TB and McS definitions applied to the earthquakes in the data base are compared. Note in Figure 9 that McS values tend to be smaller than those from TB definition.

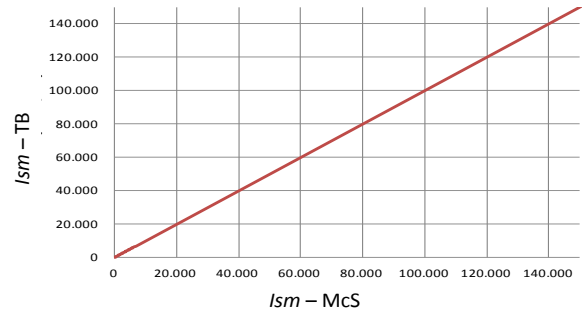


**Figure. 9 Comparing  $I_{sm}$  from TB and McS definitions of strong motion duration for the 83 records included in this article. Echezuría [1].**

With regard to VL definition of strong motion, Echezuría (2015) indicates that it yields  $a_{rms}$  values smaller (about half) than those obtained from TB definition. The  $I_{sm}$  values from both definitions, on the other hand, tend to be very close for low intensities, whereas they are slightly lower for the VL definition than the TB one for larger intensities. This is shown in Figure 10. In addition, as already mentioned, B and McS definitions of strong motion do not work well for Moment magnitudes lower than 6.5, as can be seen in Table A-1 of Appendix 1. In particular, both definitions yield duration values of a fraction of a second whereas the B one also yields values equal to zero.

As a result, the TB definition is the one closer to the new unifying criterion which will yield unique values of the duration and power as well as strong motion intensity. All those facts indicated above can also be seen in Table 1 below which includes the values of duration, root mean square of acceleration and strong motion intensity for the four definitions used in this article summarized for ranges of distance and moment Magnitude. Also note that there is a clear tendency for root mean square of acceleration and intensity of



strong motion to change with magnitude and distance for all definitions of duration.

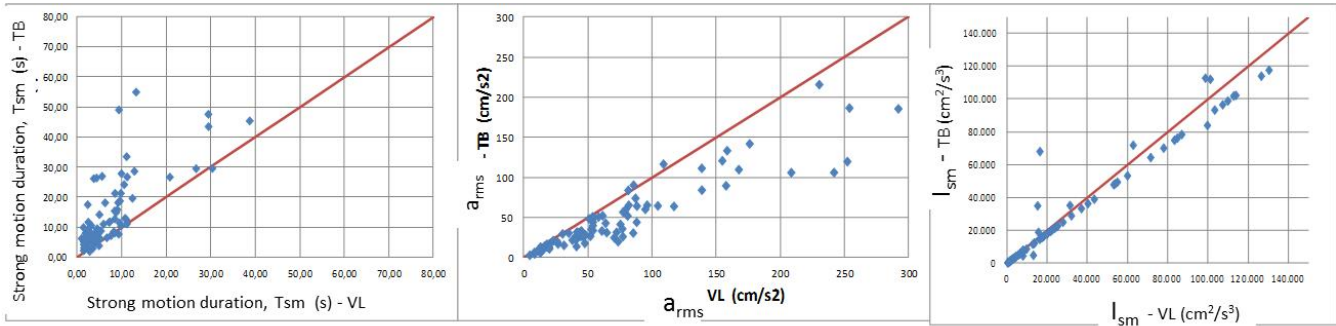


Figure. 10 Comparing  $T_{sm}$ ,  $a_{rms}$  and  $I_{sm}$  from TB and VL definitions of strong motion duration for the 83 records included in this article. Echezuría [1].

Table 1. Average values of  $T_{sm}$ ,  $a_{rms}$  and  $I_{sm}$  from the four definitions used in this article applied to the acceleration records in the data base, obtained for selected ranges of magnitude and distance.

Magnitud	Distanc	Duracoin - (segundos)				RMSA-VL (cm/s2)	RMSA-B (cm/s2)	RMSA-TB (cm/s2)	RMSA-McS (cm/s2)	Ism-VL (cm2/s3)	Ism-B (cm2/s3)	Ism-TB (cm2/s3)	Ism-McS (cm2/s3)
		V-L	B	T-B	MC-S								
5 - 5,9	0-5	3,9	3,8	5,6	2,7	64	64	52	82	18.931	19.013	19.412	15.494
	5-10	3,5	3,4	6,2	1,4	72	61	50	90	17.857	15.150	15.641	9.663
	10 -20	2,2	0,9	5,7	1,6	52	68	31	74	5.801	4.614	5.246	3.452
	20-30	4,6	0,2	6,4	4,0	17	46	12	14	997	419	913	670
6 - 6,9	0-5	3,8	12,7	7,3	5,1	200	100	126	150	136.086	135.956	124.918	120.166
	5-10	5,7	10,6	10,6	5,6	102	69	71	91	57.193	54.073	51.528	43.675
	10 -20	8,9	13,3	17,7	17,6	77	50	50	60	43.738	42.600	42.737	40.672
	20-30	7,7	6,9	17,2	11,9	49	43	30	42	17.754	13.538	15.770	15.428
	30-60	9,1	5,6	27,0	18,2	34	47	25	28	10.498	13.380	20.097	8.103
7 - 7,7	60-95	7,6	N/A	12,7	4,8	10	N/A	8	12	752	N/A	662	449
	0-10	8,7	21,6	15,7	14,9	196	133	156	163	345.466	360.377	325.792	308.161
	30-45	22,5	30,9	35,2	25,3	49	41	37	44	63.900	58.799	57.643	54.703
	85-110	20,2	13,6	33,9	21,6	32	36	22	27	23.300	17.559	21.193	18.990

The fact that the strong motion intensities are in general very close to each other for the four definitions studied indicates that all of them use a level of decreasing power along with a low increasing slope of the intensity as depicted in Figures 6 and 7. However, the criteria to establish the beginning and the end differ substantially. This also implies that all of them involve the PGA, as desired, and all what is needed is to unify the criteria to select those two points, i.e. beginning and ending of strong motion.

That unification is what the new criteria included in the next section of this article aims to. It is supported by the information included in Table 2 below in which the absolute value of the variation of the  $I_{sm}$  for each definition is included for the same ranges of moment Magnitude and distance used in Table 1. .

As noticed in Table 2 the mean variation among the different definitions of strong motion for the selected distances have in general narrow values. Most of those values are also below 25%. Notice

also that the variation values tend to increase with increasing distance.

**Table 2. Variation of the  $I_{sm}$  values for selected ranges of magnitude and distance respect to the mean of each range**

Magnitud Momento	Distanc km	Ism Mean	Absol value of Ism variation from mean			
			V-L	B	T-B	MC-S
5 - 5,9	0-5	18.213	4	4	7	15
	5-10	14.578	22	4	7	34
	10 -20	4.778	21	3	10	28
	20-30	750	33	44	22	11
6 - 6,9	0-5	129.281	5	5	3	7
	5-10	51.617	11	5	0	15
	10 -20	42.437	3	0	1	4
	20-30	15.623	14	13	1	1
	30-60	13.020	19	3	54	38
60-95	621	21	0	7	28	
7 - 7,7	0-10	334.949	3	8	3	8
	30-45	58.761	9	0	2	7
	85-110	20.260	15	13	5	6

V. NEW CRITERIA TO DEFINE THE NEW DEFINITION OF STRONG PART OF THE ACCELERATION RECORD

Based on the analyses above, a new method to define the strong section of an acceleration record was defined. It considers to initiating the exploration of the power of the record from the PGA. Then the three variables are estimated first, including accelerations to the right to the PGA and applying the criteria of intensity and power functions changes with duration. In this way the end of the strong section is identified.

Next, the same procedure is completed starting from the PGA but moving to the left of the acceleration record as the three variables are calculated. In this way the beginning of the strong part of the acceleration record is found. This ensures that maximum energy is yielded in both directions of the PGA which in turn unifies the starting and ending points of the accelerogram. The duration of the strong part is defined as the time span between the starting and ending points.

Finally, the total power of the strong part of the accelerogram is calculated starting from the beginning of the accelerogram up to the ending point. The intensity of the strong part is calculated multiplying the total power times the duration of the strong part.

Notice that this new definition and its supporting criteria satisfy the same principles regarding the strong motion definition when considering the intensity and resolves the selection of a unique starting and ending point of the strong section of the accelerogram.

VI. CHANGE OF THE INTENSITY OF THE STRONG PART OF AN ACCELEROGRAM WITH DISTANCE

As indicated above and according to Echezuría [1] the strong motion intensity decreases with moment magnitude and distance. This can be seen in Figure 11 for selected magnitude ranges using the TB definition of strong motion applied to the data in Appendix 1.

This fact will allow to estimate the demand function for problems such as liquefaction potential in terms of the conditions of the seismic province rather than using indirect means to define it, as it is currently done. This will also make it possible to estimate such liquefaction potential in probabilistic terms similar to hazard analyses for PGA and design spectra. It also means that liquefaction potential can be assessed with a probability of occurrence for a given life span considering the contribution of all source distances and magnitudes at the same time.

In order to achieve that, it will be necessary to estimate the strong motion intensity capable to generate liquefaction considering the energy required by the geotechnical conditions of a given soil deposit. Current engineering practice uses the Cyclic Stress Ratio (CSR) or Cyclic Resistance Ratio (CRR) (Seed et al (1975), fide Kramer [7]) to assess such intensity, i.e. the demand.

It is worth mentioning that it those parameters are an indirect way to estimate such demand which only take into consideration the magnitude when evaluating the energy required to liquefy a sand sample with a number of cycles of an equivalent stress amplitude. This stress amplitude is calculated using 65% of the PGA which has no connection either with the  $a_{rms}$  or with the duration in seconds or with the record power or with the strong motion intensity. In the meantime, as demonstrated above, the energy expressed in

terms of the strong motion intensity varies not only with magnitude but also with distance. Thus, this 65% used to estimate average equivalent amplitude for the PGA shall also vary with magnitude and distance.

The fact that distance is not considered in the calculation introduces another problem in the estimation of the liquefaction potential which is related to the value of the PGA to be used in the analysis. The value of the PGA depends on the distance for each source and magnitude. Some engineers use the PGA resulting from a hazard analysis but it does not provide a full behavior of the energy or strong motion intensity.

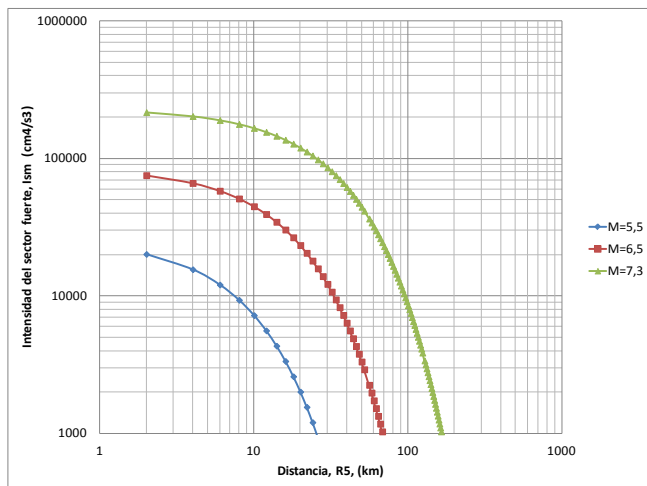


**Figure. 11** Variation of  $I_{sm}$  values from TB definition of strong motion duration with magnitude and distance for the acceleration records included in the data base.

All those inconveniences would be resolved if the energy of the quake is expressed in terms of the strong motion intensity and treated as a demand variable for which a probabilistic hazard analysis is performed. These concepts can be extended to the condition of soil improvement because the energy required to liquefy increases after treating the soil. It is then possible to express the vulnerability reduction obtained after treatment in probabilistic terms instead of only a reduction in the factor of safety.

## VII. CONCLUSIONS

A new definition of duration of the strong section of an accelerogram based on the strong motion intensity ( $I_{sm}$ ), which represents the energy of the record, the duration of the strong part of the record in seconds ( $T_{sm}$ ) and the power ( $a_{rms}^2$ ) of the record is proposed. This new definition is centered at the PGA and applies the criteria to maximize the intensity at both sides of it. This makes it easier to define both the starting and end point of the strong section.

On the other hand, considering the energy of the record in terms of the strong motion intensity demonstrates that such intensity varies with magnitude and distance. Consequently, it can be taken as a true demand variable for which probabilistic hazard techniques can be applied.

This new definition arises from the comprehensive comparison of the definitions given by TB, B, VL and McS applied to a total of 83 records from 18 earthquakes with Moment magnitude ranging from 5 to 7.7. Further, harmonic and irregular records were prepared and the same three variables mentioned above were studied to unify criteria regarding the changes of intensity and power which contribute to define the strong section of the accelerogram. This process yielded the new method to define the strong section of the acceleration record which is centered at the PGA.

The differences in criteria among the existing definitions were precisely related to the definition of both the starting and ending points of the strong section of the records. This was identified due to the fact that despite duration in seconds and root mean square of acceleration from the four definitions were significantly different between each other, the intensity calculated as the product of the power times the duration turned out to be quite close to each other. The understanding of the changes in shape of both the intensity and the power of the records made it possible to unify those criteria in a single one which yields unique values of the duration, the root mean square of the acceleration, the power and the intensity of the record.

As already mentioned, the unification of both the energy of the acceleration record and the strong motion intensity provide a new different view to a phenomenon such as liquefaction. In particular, now the definition of Cyclic Strength Ratio (CSR) and Cyclic Resistance Ratio (CRR) can be questioned as they only take into consideration the variation with magnitude. As demonstrated, the strong motion intensity varies not only with magnitude but also with distance. In the meantime, those values which represent the demand for the estimation of liquefaction potential are obtained from indirect analyses using laboratory data on sand specimens rather than taking into consideration the seismic province, i.e. location and length of faults, seismic generation capacity and recurrence among others. All these aspects which allow to consider the strong motion intensity as a true demand variable make possible the unification of the strong part of the acceleration record.

#### REFERENCIAS

- [1] Echezuría, H., 2015, "Comparing Ground Motion Intensity, Root Mean Square of Acceleration and Time Duration from Four Definitions of Strong Motion" The Open Civil Engineering Journal, 9, 1-14.
- [2] Vanmarcke, E. H. and Lai, S. P., 1980, "Strong motion duration and RMS amplitude of earthquake records", Bull. Seism. Soc. Am. , V.70, No 4, Aug., pp 1293-1307.
- [3] Bolt, B. A., 1973, "Duration of strong ground motion" Proc. 5th World Conf. on Earthq. Eng. Vol.1, Rome.
- [4] Trifunac, M. B. and Brady, G., 1975, "A study on the duration of strong earthquake ground motion" Bull. Seism. Soc. Am. V.5, No. 3, June, pp 581-626.
- [5] Mc Cann, M., 1980, "RMS acceleration and duration of strong ground motion", The John A Blume Earthq. Eng. Center, Report No 46, Stanford University,.
- [6] Arias, A., 1970 "A measure of earthquake intensity", Seismic Design of Nuclear Power Plants, Hansen, R., edit. MIT Press, Cambridge, Mass..
- [7] Kramer, S. L., 1996, *Geotechnical Earthquake Engineering*, Prentice Hall.
- [8] Echezuría, H., 2017, "Cambios en las intensidades del sector fuerte del acelerograma para cuatro definiciones de duración", XI Congreso Venezolano de Sismología, CONVESIS, Julio.

**Appendix 1**

**Table A-1 Earthquakes used in this study**

	Earthquake Name & date	Magnitude Moment	Distance (km)	Duration - (seconds)				PGA (cm/s <sup>2</sup> )	RMSA-VL (cm/s <sup>2</sup> )	RMSA-B (cm/s <sup>2</sup> )	RMSA-TB (cm/s <sup>2</sup> )	RMSA-McS (cm/s <sup>2</sup> )
				V-L	B	T-B	MC-S					
1	Tabas (Iran) - 78	7,7	3,00	8,93	24,48	16,06	14,10	786,16	253,53	159,38	186,87	196,07
2	San Fernando - 71	6,6	20,50	10,69	9,26	13,20	5,80	212,12	61,28	62,55	52,45	74,13
3	San Fernando - 71	6,6	54,00	13,16	0,00	55,16	61,40	42,4	12,72	0,00	5,89	5,80
4	San Fernando - 71	6,6	82,00	6,20	0,00	18,36	1,40	37,37	8,28	0,00	4,71	10,54
5	San Fernando - 71	6,6	59,00	8,36	0,20	12,98	5,60	76,93	17,67	76,63	13,45	16,94
6	San Fernando - 71	6,6	66,00	4,70	0,00	9,30	0,80	55,94	15,02	0,00	10,19	22,51
7	San Fernando - 71	6,6	29,60	8,35	5,80	15,68	3,20	147,18	43,92	36,40	30,46	54,62
8	San Fernando - 71	6,6	27,60	9,13	9,87	18,42	13,00	147,22	41,24	35,79	31,97	38,86
9	San Fernando - 71	6,6	22,50	10,94	8,14	12,76	11,60	111,89	34,85	36,73	30,74	32,44
10	San Fernando - 71	6,6	18,40	7,50	6,72	7,42	4,60	200,22	53,49	54,17	51,01	59,53
11	San Fernando - 71	6,6	64,00	8,15	0,00	8,74	5,20	27,48	8,15	8,15	6,56	7,61
12	San Fernando - 71	6,6	91,00	9,24	0,00	7,94	6,60	38,28	12,91	0,00	13,21	13,67
13	Borrego Mount - 68	6,6	45,00	9,31	9,96	49,24	26,60	139,37	40,29	66,90	26,63	21,99
14	Daily City - 57	5,2	3,45	3,45	0,38	3,22	1,20	124,65	30,05	48,24	29,70	37,89
15	Imperial Valley - 40	7	10,00	10,47	29,30	24,40	25,20	352,34	104,25	61,45	64,75	65,57
16	Lyttle Creek - 70	5,3	18,00	4,44	1,10	5,48	0,20	84,41	20,44	35,19	17,69	34,72
17	Lyttle Creek - 70	5,3	18,00	2,79	0,04	2,78	0,60	75,29	22,82	75,29	21,37	25,24
18	Lyttle Creek - 70	5,3	29,00	9,76	0,00	10,60	2,00	44,17	12,18	0,00	11,30	17,29
19	Parkfield - 66	6,1	63,00	9,52	0,00	18,98	10,20	17,67	4,52	0,00	3,04	3,83
20	Parkfield - 66	6,1	5,50	2,76	7,30	6,72	2,20	458,34	138,60	82,85	84,34	108,33
21	Parkfield - 66	6,1	9,60	3,06	7,62	10,86	4,00	273,83	87,79	52,11	44,25	63,82
22	Parkfield - 66	6,1	14,90	9,86	0,56	28,06	70,67	70,67	19,77	29,32	11,14	11,27
23	Parkfield - 66	6,1	0,08	4,72	12,08	6,96	2,00	716,46	154,51	95,62	121,00	200,06
24	Kern County - 52	7,4	109,00	26,64	0,14	29,72	17,80	55	16,26	54,74	14,70	17,97
25	Kern County - 52	7,4	42,00	12,78	15,56	28,84	10,20	193,35	53,73	44,66	33,96	51,07
26	Kern County - 52	7,4	85,00	11,03	9,00	33,70	14,40	132,5	40,43	36,37	21,96	28,87
27	Coyote Lake - 79	5,8	8,90	4,20	1,59	5,97	3,40	127,59	43,11	46,39	27,15	33,79
28	Coyote Lake - 79	5,8	8,00	4,84	5,23	4,08	1,10	355,18	81,22	75,52	84,11	146,51
29	Coyote Lake - 79	5,8	5,30	3,87	5,24	8,35	1,00	264,99	80,71	63,58	52,22	118,80
30	Coyote Lake - 79	5,8	4,90	4,69	7,12	8,20	6,30	255,18	81,61	70,60	65,51	73,24
31	Coyote Lake - 79	5,8	3,90	3,55	3,86	5,48	0,60	225,73	79,51	73,17	60,72	135,19
32	Imperial Valley - 79	6,5	0,20	3,47	10,36	4,78	3,60	510,36	175,80	100,46	142,11	160,50
33	Imperial Valley - 79	6,5	1,40	3,92	10,53	8,17	5,20	706,65	167,38	100,07	110,00	127,10
34	Imperial Valley - 79	6,5	2,80	4,40	18,87	9,76	10,10	794,98	291,63	140,20	185,85	187,10
35	Imperial Valley - 79	6,5	3,50	1,57	9,61	5,83	4,10	628,13	251,89	97,25	120,00	144,00
36	Imperial Valley - 79	6,5	1,00	1,77	15,44	8,26	4,80	549,62	241,54	81,51	106,30	132,50
37	Imperial Valley - 79	6,5	4,40	1,92	11,14	6,64	5,10	598,96	208,20	84,92	106,20	119,60
38	Imperial Valley - 79	6,5	12,20	5,27	11,57	9,00	5,30	372,95	138,47	101,70	111,59	140,10
39	Imperial Valley - 79	6,5	9,30	9,46	12,59	11,69	5,40	264,99	86,87	73,28	74,20	103,00
40	Imperial Valley - 79	6,5	10,20	2,53	12,16	8,91	5,00	422,03	157,40	79,21	89,83	111,80
41	Imperial Valley - 79	6,5	18,00	12,34	17,94	19,83	18,00	147,22	44,65	35,12	33,42	35,12
42	Imperial Valley - 79	6,5	21,50	8,42	8,82	21,50	15,50	147,22	44,44	37,72	26,66	30,62
43	Imperial Valley - 79	6,5	16,40	8,68	10,44	15,14	5,30	147,22	44,71	38,14	32,17	47,19
44	Imperial Valley - 79	6,5	7,00	4,92	11,55	14,41	11,20	215,92	75,10	46,84	41,61	44,86
45	Imperial Valley - 79	6,5	7,30	7,09	12,39	11,89	6,80	255,18	87,95	64,56	64,43	81,95
46	Imperial Valley - 79	6,5	10,10	5,84	12,98	11,25	7,30	274,81	95,94	62,69	65,59	76,45
47	Imperial Valley - 79	6,5	13,10	2,29	5,28	17,74	5,28	196,29	76,98	41,76	26,26	36,77
48	Imperial Valley - 79	6,5	22,20	4,27	1,91	26,60	29,30	127,59	47,37	44,73	17,98	17,86
49	Imperial Valley - 79	6,5	24,50	2,42	4,59	11,90	4,90	206,11	73,30	48,64	20,01	47,08
50	Imperial Valley - 79	6,5	30,50	11,09	2,18	11,34	10,30	68,7	17,82	22,98	16,72	17,34
51	Imperial Valley - 79	6,5	5,10	5,05	12,48	6,39	4,50	500,54	158,24	99,51	133,56	153,20
52	Imperial Valley - 79	6,5	8,20	7,27	10,21	12,03	5,10	225,73	77,19	62,23	56,92	79,83
53	Imperial Valley - 79	6,5	19,10	30,29	32,79	29,77	31,10	116,85	50,70	47,36	48,53	48,22
54	Imperial Valley - 79	6,5	12,80	9,73	21,98	21,52	21,20	264,99	94,48	60,82	60,36	62,85
55	Imperial Valley - 79	6,5	18,80	3,66	13,67	26,40	19,40	186,48	70,29	2,00	24,91	28,47
56	Imperial Valley - 79	6,5	37,00	5,51	8,53	27,16	8,70	157,03	54,31	37,75	50,04	37,32

Table continues on next page

Table A-1 Earthquakes used in this study (cont)

	Earthquake Name & date	Magnitude Moment	Distance (km)	Duration - (seconds)				PGA (cm/s <sup>2</sup> )	RMSA-VL (cm/s <sup>2</sup> )	RMSA-B (cm/s <sup>2</sup> )	RMSA-TB (cm/s <sup>2</sup> )	RMSA-McS (cm/s <sup>2</sup> )
				V-L	B	T-B	MC-S					
57	Imp Val- Aftershok - 79	5	25,90	1,48	0,13	3,31	3,90	55,94	19,41	45,67	12,16	10,84
58	Imp Val- Aftershok - 79	5	14,10	2,78	0,44	10,15	5,55	95,2	31,14	62,06	15,46	14,99
59	Imp Val- Aftershok - 79	5	18,90	1,68	0,89	5,61	0,30	151,14	51,75	64,42	26,85	86,49
60	Imp Val- Aftershok - 79	5	16,50	1,93	0,43	5,13	0,35	144,27	45,95	87,25	26,73	91,54
61	Imp Val- Aftershok - 79	5	12,60	1,38	1,13	6,43	0,20	232,61	72,08	72,07	31,69	147,42
62	Imp Val- Aftershok - 79	5	11,90	0,92	0,85	6,47	0,25	280,7	85,12	77,12	30,77	120,13
63	Imp Val- Aftershok - 79	5	11,30	1,40	0,97	5,37	0,30	225,73	64,45	72,25	31,28	90,14
64	Imp Val- Aftershok - 79	5	12,60	1,48	1,04	4,43	0,55	130,53	60,67	68,33	33,36	83,59
65	Imp Val- Aftershok - 79	5	13,90	2,81	0,02	5,99	5,95	510,91	19,26	70,91	12,51	12,54
66	Imp Val- Aftershok - 79	5	16,20	1,83	0,92	3,60	0,50	188,44	63,57	83,62	43,08	100,52
67	Imp Val- Aftershok - 79	5	11,70	3,10	1,63	7,22	0,40	144,27	45,29	53,59	28,17	71,75
68	Imp Val- Aftershok - 79	5	10,30	1,43	1,40	5,82	0,70	259,1	76,57	72,68	36,02	98,27
69	Imp Val- Aftershok - 79	5	14,60	1,34	0,02	10,13	9,75	126,61	40,87	69,28	14,01	14,53
70	Imp Val- Aftershok - 79	5	11,20	2,73	1,92	2,18	0,70	258,12	85,39	98,30	90,58	134,87
71	Imp Val- Aftershok - 79	5	11,90	1,81	1,09	4,68	0,30	154,09	47,90	53,21	28,34	83,85
72	Imp Val- Aftershok - 79	5	24,90	2,58	0,26	5,30	6,05	58,89	19,54	46,67	13,00	12,56
73	Hollister - 74	5	10,80	1,40	1,08	2,46	1,20	137,4	42,80	44,48	31,65	42,03
74	Hollister - 74	5	10,80	4,63	2,00	9,18	1,00	166,85	52,37	68,84	35,46	83,80
75	Hollister - 74	5	8,90	3,02	1,54	8,06	1,00	117,77	37,65	41,21	21,88	41,21
76	Sitka Alaska - 72	7,7	45,00	11,15	12,26	26,94	12,80	107,96	26,53	22,62	17,17	22,75
77	Managua-Nicaragua - 72	6,1	5,00	8,35	13,26	8,26	6,20	382,77	108,68	96,11	116,84	132,43
78	Gazly (USSR) - 76	7	3,50	6,59	11,14	6,73	5,26	794,94	230,00	176,91	216,09	228,27
79	St. Elias (Alka) - 79	7,6	38,30	20,74	17,58	26,90	17,10	157,03	53,72	54,04	44,49	54,36
80	St. Elias (Alka) - 79	7,6	96,60	29,43	15,49	43,69	37,69	88,33	25,86	25,91	20,13	20,52
81	Lima - Peru - 76	7,6	38,00	29,39	53,72	47,80	43,40	255,55	53,65	38,64	39,91	41,31
82	Lima - Peru - 76	7,6	40,00	38,67	55,44	45,60	43,20	245,36	58,05	47,51	50,79	51,75
83	Sta. Barbara - 41	5,9	10,00	1,47	3,24	4,46	0,40	235,55	116,82	75,98	64,08	111,91